J Am Soc Nephrol 10: 2146–2157, 1999

Transglutaminase Transcription and Antigen Translocation in Experimental Renal Scarring

TIMOTHY S. JOHNSON,* N. JAMES SKILL,† A. MEGUID EL NAHAS,* SIMON D. OLDROYD,* GRAHAM L. THOMAS,* JULIE A. DOUTHWAITE,* JOHN L. HAYLOR,* and MARTIN GRIFFIN†

**Sheffield Kidney Institute, Northern General Hospital Trust, Sheffield, and †Department of Life Sciences, Nottingham Trent University, Nottingham, United Kingdom.*

Abstract. It was recently demonstrated that renal tissue transglutaminase (tTg) protein and its catalytic product the ε(γ-glutamyl) lysine protein cross-link are significantly increased in the subtotal (5/6) nephrectomy model (SNx) of renal fibrosis in rats. It was proposed that the enzyme had two important physiologic functions in disease development; one of stabilizing the increased extracellular matrix (ECM) by protein cross-linking, the other in a novel form of tubular cell death. This study, using the same rat SNx model, demonstrates first by Northern blotting that expression of tTg mRNA when compared with controls is increased by day 15 (+70% increase, $P < 0.05$), then rises steadily, peaking at day 90 (+391%, $P < 0.01$), and remains elevated at 120 d (+205%, $P < 0.05$) when compared with controls. *In situ* hybridization histochemistry demonstrated that the tubular cells were the major site of the additional tTg synthesis. Immunohistochemistry on cryostat sections revealed a sixfold increase ($P < 0.001$) in ECM-bound tTg antigen at 90-d post-SNx, whereas *in situ* transglutaminase activity demonstrated by the incorporation of fluorescein cadaverine into cryostat sections indicated a 750% increase ($P < 0.001$) on day 90 in SNx animals. This increased activity was extracellular and predominantly found in the peritubular region. These results indicate that increased tTg gene transcription by tubular cells underlies the major changes in renal tTg protein reported previously in SNx rats, and that the presence of the ε(γ-glutamyl) lysine cross-links in the extracellular environment is the result of the extracellular action of tTg. These changes may be in response to tubular cell injury during the scarring process and are likely to contribute to the progressive expansion of the ECM in renal fibrosis.

The progression of chronic renal insufficiency is characterized by a relentless fibrosis of the kidney. This is typically described as an accumulation of the extracellular matrix (ECM) above normal requirements and a loss of specialized renal cells and architecture. Increased synthesis and decreased breakdown of the renal ECM have been implicated in its expansion (1,2). The latter may be due to changes in the ECM-regulating enzymes including a fall in renal matrix metalloproteinases (MMP) and plasminogens or an increase in their inhibitors (tissue inhibitors of matrix metalloproteinases and plasminogen activator inhibitors) (3–5). Other factors important in the pathogenesis of renal fibrosis that have thus far received little attention are those contributing to the increased deposition and stabilization of the ECM, thereby increasing its resistance to enzymatic breakdown. Such a proposal has been put forward as a contributing factor in the development of other fibrogenic processes including lung and liver fibrosis as well as atherosclerosis (6–10). We have recently described (11) the expression of tissue transglutaminase (tTg) in the 5/6 subtotal nephrectomy (SNx) model of renal fibrosis in which the cross-linking of the ECM by tTg and the formation of irreversible ε(γ-glutamyl) lysine bonds may underlie its resistance to breakdown. Furthermore, the intracellular consequence of high tTg and its product in the scarred kidney was hypothesized to be a novel type of transglutaminase-mediated cell death whereby the cross-linking of intracellular proteins in the cell leads to its death. Transglutaminase-mediated cell death has since been confirmed as a distinct biologic process in a hamster fibrosarcoma cell line in response to dexamethasone induction of tTg in the absence of any increase in apoptosis (12) and in tTg transfected 3T3 fibroblasts after exposure to ionomycin (13). The ability of the enzyme to not only stabilize ECM proteins but also to be a key player in a novel cell death process represents a major step in improving our understanding of the mechanisms of tissue fibrosis.

Transglutaminases are calcium-dependent enzymes that catalyze the posttranslation modification of proteins through an acyl transfer reaction between the carboxamide group of a peptide-bound glutaminyl residue and various primary amines (14). Covalent cross-links using ε(γ-glutamyl) lysine bonds are stable and resistant to enzymatic, chemical, and mechanical disruption (14). Endopeptidases capable of hydrolyzing the ε(γ-glutamyl) lysine cross-links formed by transglutaminases (Tg) have not been described in vertebrates, and even lysosomes do not contain enzymes capable of splitting the ε(γ-

Received January 28, 1999. Accepted April 18, 1999.
Correspondence to Dr. Martin Griffin, Department of Life Sciences, Nottingham Trent University, Clifton, Nottingham, NG11 8NS, United Kingdom. Phone: +44 (0)115 9486670; Fax: +44 (0)115 9486636; E-mail: martin.griffin@ntu.ac.uk
1046-6673/1010-2146
Journal of the American Society of Nephrology

glutamyl) lysine bonds (15–17). A number of Tg enzymes have been characterized that have distinct genes, structures, and physiologic functions. Examples include the plasma factor XIIIa involved in cross-linking fibrin during wound healing (18) and the keratinocyte transglutaminase involved in the formation of the cornified envelope during terminal differentiation (19,20). tTg is the most widespread member of this family and is present in many different cell types.

Recent evidence suggests that the tTg may have a number of key functions in cells. These include a role in programmed cell death (21–23), cell adhesion (24), and interactions between the cell and its ECM via the cross-linking of proteins such as fibronectin, laminin, nidogen, and collagen types I, III, and IV (7,13,25–27). In addition, tTg has recently been demonstrated to play a role in the covalent stabilization of collagen fibrillar formation through cross-linking of the core fibrils (28).

Previous investigations in renal fibrosis have demonstrated that the product of tTg, $\epsilon(\gamma$-glutamyl) lysine cross-link, is present both in the extracellular space and in the cytoplasm of tubular cells during the scarring progress (11), whereas elevated tTg can only be found intracellularly. This raised the question of whether ECM components were being cross-linked internally before secretion or, as noted previously, whether the tTg antigen present in the matrix is difficult to detect because of occlusion of the epitope by standard fixation techniques (13). In addition, there is only circumstantial evidence that elevated tTg cross-linking of ECM components affects the resistance of these proteins to the catalytic action of MMP. Although we demonstrated previously that enzyme activity is increased by virtue of the presence of increased amounts of the $\epsilon(\gamma$-glutamyl) lysine cross-link product in renal scarring, no claim was made as to whether this increase in activity was a result of *de novo* synthesis of the enzyme, or, alternatively, the activation of a latent proenzyme (29,30) as proposed previously following wound healing in skin (31).

In this study, we demonstrate that induction of renal fibrosis in rats using the SNx model leads to *de novo* synthesis of tTg by the renal tubular cells. Moreover, by using cryostat rather than fixed tissue sections, we show that there is increased amounts of tTg antigen present in the intercellular space of the renal tubules, which, by using a novel *in situ* activity method, we demonstrate to be active after progression of the fibrotic disease. In keeping with the importance of tTg in the stabilization of ECM proteins, we also demonstrate the increased resistance of tTg cross-linked ECM proteins to the action of MMP.

Materials and Methods

Experimental Animals and Protocol

Male Wistar rats (Sheffield University strain) of approximately similar weight (350 to 400 g) and age (8 to 10 wk) were subjected to SNx by complete removal of the left kidney and upper and lower pole resections of the right kidney. Rats were housed two to four to a cage and were maintained at 20°C and 45% humidity on a 12-h light/dark cycle. They were allowed free access to standard rat chow (Labsure, March, Cambridge, United Kingdom) and tap water. At days 7, 15, 30, 60, 90, and 120 post-SNx, experimental groups of five to six rats were sacrificed and the remnant kidney was removed. At each time point, five to six control animals were also sacrificed that had been subjected to a sham operation. Before sacrifice, renal function (serum creatinine and creatinine clearance) and proteinuria were measured in all rats. Creatinine was measured by the standard autoanalyzer technique and proteinuria by the biuret method. All procedures were carried out under license according to regulations laid down by Her Majesty's Government, United Kingdom (Animals Scientific Procedures Act, 1986).

Assessment of Renal Scarring

Analysis of renal scarring was determined on formal calcium-fixed, paraffin-embedded sections (4 μm) stained by hematoxylin and eosin or Masson's trichrome. One of the authors (G.L.T.) scored the severity of glomerulosclerosis and tubulointerstitial scarring, blinded to their code, according to a previously described 4-point arbitrary score (11). An overall renal fibrosis score was determined by taking a mean of glomerulosclerosis and tubulointerstitial scores. Scores were attributed as follows:

Glomerulosclerosis Score (0 to 3). 0, normal glomeruli; 1, presence of mild segmental glomerulosclerosis affecting $<25\%$ of the glomerular tuft; 2, moderate segmental sclerosis affecting 25 to 50% of the tuft; 3, diffuse severe glomerulosclerosis affecting $>50\%$ of the tuft including glomeruli with total tuft obliteration, fibrosis, and obsolescence. A minimum of 25 glomeruli per kidney per remnant kidney was examined, and the mean of the glomerular scores was taken to represent the severity of glomerulosclerosis for a given rat (11).

Tubulointerstitial Scarring (1 to 4). 0, normal tubules and interstitium; 1, mild tubular atrophy and interstitial fibrosis; 2, moderate tubular atrophy and dilation with marked interstitial fibrosis; 3, end-stage kidney with extensive interstitial fibrosis and few remaining atrophic tubules. A score was given to each microscopic field viewed at a magnification of $\times 200$. A minimum of 10 fields was scored per kidney per remnant kidney, and the mean value was taken to represent the tubulointerstitial score for a given rat (11).

tTg mRNA Levels

tTg mRNA levels were determined by Northern blot analysis. Total RNA was extracted using Trizol™ (Life Technologies BRL, Paisley, United Kingdom) and quantified by both optical density at 260 nm and ultraviolet (UV) densitometry of the 18S rRNA subunit. Fifteen micrograms of total RNA was then run on a 1.2% (wt/vol) agarose/4-morpholinepropanesulfonic acid/formaldehyde gel and then capillary-blotted on to Hybond-N (Amersham, Buckinghamshire, United Kingdom) and cross-linked with 70 mJ/cm^2 UV radiation (UV cross-linker, Amersham). This was then probed with a ^{32}P-dCTP random-primed (Prime-A-Gene, Promega, United Kingdom) tTg-specific DNA probe corresponding to a 385-bp *Bam*HI fragment of the complete mouse tTg sequence extending from bp 1240 to 1625 of the coding region. This was then exposed to Biomax MS film for approximately 4 h. The resulting autoradiograph was then quantified by scanning densitometry using a Bio-Rad GS-690 densitometer and Molecular Analyst version 4 software. Transcript size was determined by comparison to RNA molecular weight markers (Promega) using the same analysis package. Values were then corrected for loading using repeat probings with the housekeeping genes cyclophilin and β-actin. Regulation failure of housekeeping genes was by comparison with the 18S rRNA subunit on ethidium bromide-stained gels.

tTg mRNA Location

tTg mRNA location was determined by *in situ* hybridization. Five-micromolar sections of 10% neutral-buffered, formalin-fixed, paraffin-embedded tissue on aminopropyltriethoxysilane-coated slides were rehydrated, treated with 5 mM levamisole, and 0.2N hydrochloric acid for 20 min and then digested with 5 μg/ml proteinase K (Sigma, Poole, United Kingdom) for 60 min at 37°C. They were then post-fixed in 1% paraformaldehyde, washed, and dehydrated. These were then probed with sense and antisense riboprobe constructs to tTg constructed using digoxigenin-labeled rUTP and generated from the same tTg cDNA sequence used above using the riboprobe Gemini II system (Promega). Hybridization was performed at 50°C for 18 h in 50% (vol/vol) deionized formamide, 5 mM ethylenediaminetetraacetic acid (EDTA), 10 mM NaH_2PO_4, 0.2 mg/ml herring sperm DNA (Promega), 0.1 mg/ml yeast tRNA (Sigma), 2× SSC, 1× Denhardt's solution, and 10% dextran sulfate containing 10 ng/ml digoxigenin-labeled riboprobe. After stringency washes, any nonduplexed RNA was digested with 20 μg/ml RNase A (Sigma) for 30 min at 37°C. Binding of the riboprobes was then revealed using alkaline phosphatase-conjugated sheep anti-digoxigenin antibody (Boehringer Mannheim, UK) diluted 1:500 (1.5 U/ml) in TBS containing 1% (vol/vol) normal sheep serum for 60 min at room temperature, followed by addition of a color substrate solution consisting of 4-nitroblue tetrazolium chloride/5-bromo-4-chloro-3-indolyl phosphate. The color reaction was developed in the dark at 37°C and stopped with distilled water and mounted under aqueous mounting medium (60% [vol/vol] glycerol).

tTg Immunohistochemistry using Cryostat Sections

Kidney tissue was snap-frozen in liquid nitrogen and then mounted in OCT mounting media (Raymond Lamb, United Kingdom). Ten-micrometer cryostat sections were cut at −12°C and placed onto low iron clear glass slides (Raymond Lamb) and stored at −20°C before use.

All solutions before fixation were supplemented with the protease inhibitors 1 mM leupeptin, 1 mM benzamidine, 1 mM pepstatin, 1 mM phenylmethylsulfonyl fluoride, and 10 mM EDTA. Sections were thawed by adding blocking media, washed, and then blocked for 1 h at room temperature with blocking media (3% bovine serum albumin, 0.01% Triton X-100 in phosphate-buffered saline [PBS] at pH 7.4) to which was added 5% (vol/vol) goat serum to absorb out any tTg released from damaged cells during hydration. Sections were then washed with PBS and either a 1:300 dilution of a mouse monoclonal anti-tTg antibody (CUB7042) (Stratech Scientific, Luton, United Kingdom) or mouse nonimmune serum (Dako, UK) applied to the sections and incubated overnight at 4°C. Sections were washed with PBS and then fixed with cold methanol (−20°C) for 10 min. These were then washed in PBS before addition of a 1:500 dilution of a goat anti-mouse Cy5 (indodicarbocyanine)-conjugated antibody (Stratech Scientific) and incubation for 1 h at room temperature. Sections were then washed in PBS and mounted with vector shield fluorescence mounting media (Vector Laboratories, Peterborough, United Kingdom).

Sections were visualized using a Leica TCS NT confocal microscope (Leica DMRBE; Lasertechnik, Wetzlar, Germany) using a

Table 1. Renal function and scarring of subtotal 5/6 nephrectomy (SNx) kidneys

Days post-SNx	Body Weight (g)	Serum Creatinine (μmol/L)	Creatinine Clearance (ml/min)	Proteinuria (mg/24 h)	Scarring Index
7					
SNx ($n = 6$)	331 ± 5.7	68.5 ± 5.8	0.81 ± 0.06	16.8 ± 4.5	0.22 ± 0.10 (G) 0.31 ± 0.13 (T)
sham ($n = 6$)	414 ± 11.0	33.8 ± 3.1	1.60 ± 0.29	6.5 ± 0.7	
15					
SNx ($n = 5$)	322 ± 6.9	84.2 ± 7.9	0.65 ± 0.08	16.7 ± 2.8	0.18 ± 0.06 (G) 0.28 ± 0.06 (T)
sham ($n = 5$)	387 ± 2.2	42.6 ± 2.4	1.08 ± 0.01	9.3 ± 2.7	
30					
SNx ($n = 6$)	402 ± 16.1	78.7 ± 6.4	0.86 ± 0.08	40.4 ± 8.8	0.34 ± 0.05 (G) 0.54 ± 0.06 (T)
sham ($n = 5$)	395 ± 22.3	52.6 ± 3.4	1.43 ± 0.14	7.9 ± 1.5	
60					
SNx ($n = 5$)	404 ± 23.3	107.4 ± 28.5	0.67 ± 0.13	131.1 ± 23.0	0.73 ± 0.12 (G) 1.18 ± 0.25 (T)
sham ($n = 5$)	455 ± 13.0	43.2 ± 1.6	1.30 ± 0.13	6.9 ± 1.8	0.02 ± 0.02 (T)
90					
SNx ($n = 5$)	424 ± 12.1	111.2 ± 19.9	0.76 ± 0.12	234.1 ± 45.2	1.67 ± 0.16 (G) 1.73 ± 0.20 (T)
sham ($n = 5$)	499 ± 19.6	53.4 ± 5.6	1.65 ± 0.22	9.9 ± 1.1	
120					
SNx ($n = 5$)	448 ± 6.3	140.6 ± 36.5	0.76 ± 0.25	256.8 ± 56.8	1.86 ± 0.15 (G) 1.93 ± 0.24 (T)
sham ($n = 5$)	498 ± 9.8	40.0 ± 1.6	2.08 ± 0.27	7.4 ± 0.8	

Kr/AR laser (647 and 488 nm) for both Cy5 (optimal excitation 650 nm) and autofluorescence. Computer imaging and analyses were obtained at 665 and 530 nm for Cy5 and autofluorescence, respectively (Leica TCS NT, Lasertechnik).

Tg in Situ Activity Assay

The method is a modification of that used previously for detection of *in situ* Tg activity of cells in live culture (13). Cryostat sections were prepared as described above. All solutions before fixation were supplemented with the protease inhibitors as described above. Fifty microliters of 0.2 mM fluorescein cadaverine (32) (Molecular Probes, Leiden, The Netherlands), 50 mM Tris-HCl, pH 7.4, and either 10 mM $CaCl_2$ or 10 mM EDTA was pipetted on to a section and incubated for 1 h at 37°C in a humidity chamber. As additional negative controls to EDTA, some sections were also preincubated for 5 min with 10 mM cystamine (Tg inhibitor) or with the inactivating tTg antibody (CUB7402 purified IgG) dilution 1:50. To verify that available endogenous Tg substrates were not a limiting factor, 50 μg of tTg was included in the reaction buffer as a positive control. Sections were then washed in Tris-HCl, pH 7.4, and then fixed with −20°C methanol for 10 min. The methanol was allowed to evaporate and the section was then blocked for 1 h at room temperature with antibody dilution buffer (3% bovine serum albumin, 0.01% Triton X-100 in PBS, pH 7.4) containing 5% (vol/vol) goat serum. After PBS washes, the sections were probed with 50 μl of a 1:50 dilution of mouse anti-FITC monoclonal antibody (Sigma) at 4°C overnight. Sections were then washed again with PBS, and 50 μl of a 1:500 dilution of goat anti-mouse, Cy5-conjugated antibody (Stratech Scientific) was applied for 1 h at room temperature. Finally, sections were washed in PBS and mounted using vector shield fluorescence mounting media (Vector Laboratories).

Sections were visualized using confocal microscopy (Leica DMRBE, Leica), using Kr/AR laser (647 and 488 nm) for both Cy5 (optimal excitation 650 nm) and FITC (optimum excitation 494 nm). Computer imaging and analyses were obtained at emission wavelengths of 665 and 530 nm for Cy5 and FITC, respectively (Leica TCS NT). Antibody binding to the FITC was shown to quench emissions from the FITC cadaverine conjugate such that emissions at 530 nm were predominantly due to the autofluorescence of the tissue.

Measurement of the Effect of tTg Cross-Linking on MMP Activity

This was undertaken using a modification of the collagen fibril assay of Werb and Burleigh (33). Briefly, ^{3}H-labeled collagen (New England Nuclear, United Kingdom) with a specific activity of 925 GBq/mmol was added to 1 mg/ml solution of purified collagen type 1 (Sigma) in 0.01 M acetic acid, until the dpm were equivalent to 2500 dpm per μl. An equal volume of 40 mM Tris, 100 mM NaCl, 20 mM $CaCl_2$, and 20 mM dithiothreitol was then added. This was supplemented with either 10 μg/ml tTg (Sigma), 10 μg/ml tTg plus 100 μg/ml fibronectin (Life Technologies BRL), or PBS. This was then left for 3 h at 37°C for collagen fibril formation to occur, after which a small volume was removed and centrifuged at 10,000 × *g* to pellet the collagen fibril clot, and then the incorporation of labeled collagen was determined. To the remaining fibril solution, semipurified and activated MMP-1 was added to 1 μg/ml and incubated for an additional 16 h at 37°C. This was then centrifuged as before and the amount of solubilized collagen was determined. To verify that tTg was not cross-linking MMP and thus reducing its activity, controls were undertaken by adding the tTg inhibitor cystamine (34) before MMP addition. Inhibition of tTg activity was confirmed by the use of the [^{14}C]-putrescine incorporation into N_1N^1-dimethylcasein assay for Tg activity (29). MMP activity at the end of the assay was determined by gelatinase zymography (35) and by assays using the fluorogenic MMP substrate Dnp-Pro-Leu-Gly-Cys(Me)-His-Ala-D-Arg-NH_2 (Bachem Ltd., Essex, United Kingdom) (36).

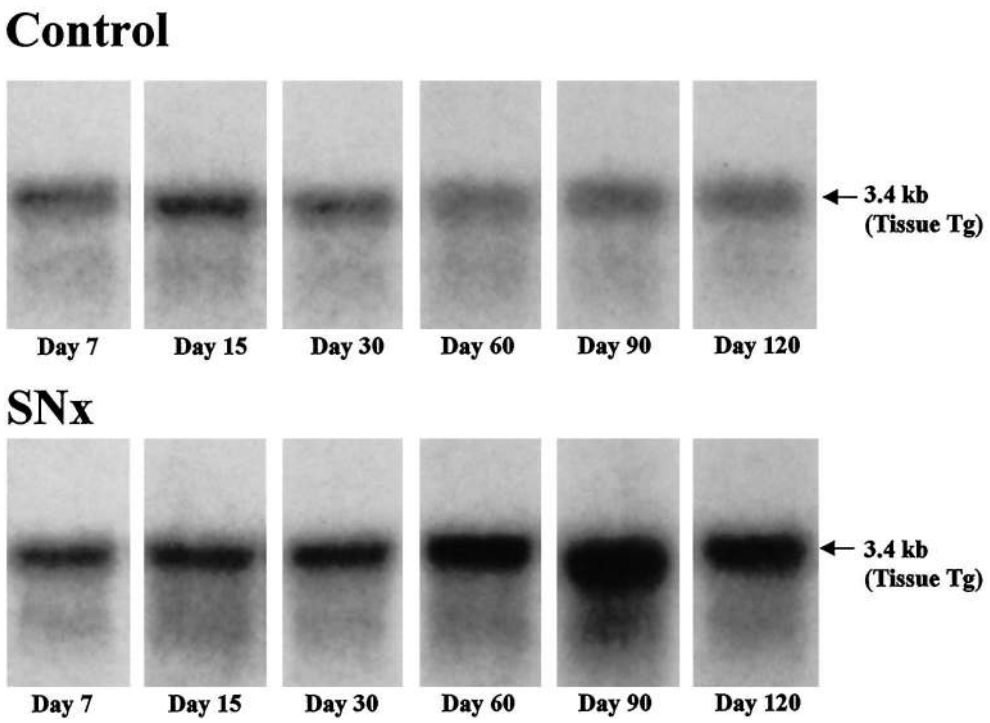

Figure 1. A Northern blot of total RNA from control and 5/6 subtotal nephrectomy (SNx) kidneys over a 120-d time course probed with a ^{32}P random-primed DNA probe specific for tissue transglutaminase (tTg). Representative panels are shown. $n \geq 5$.

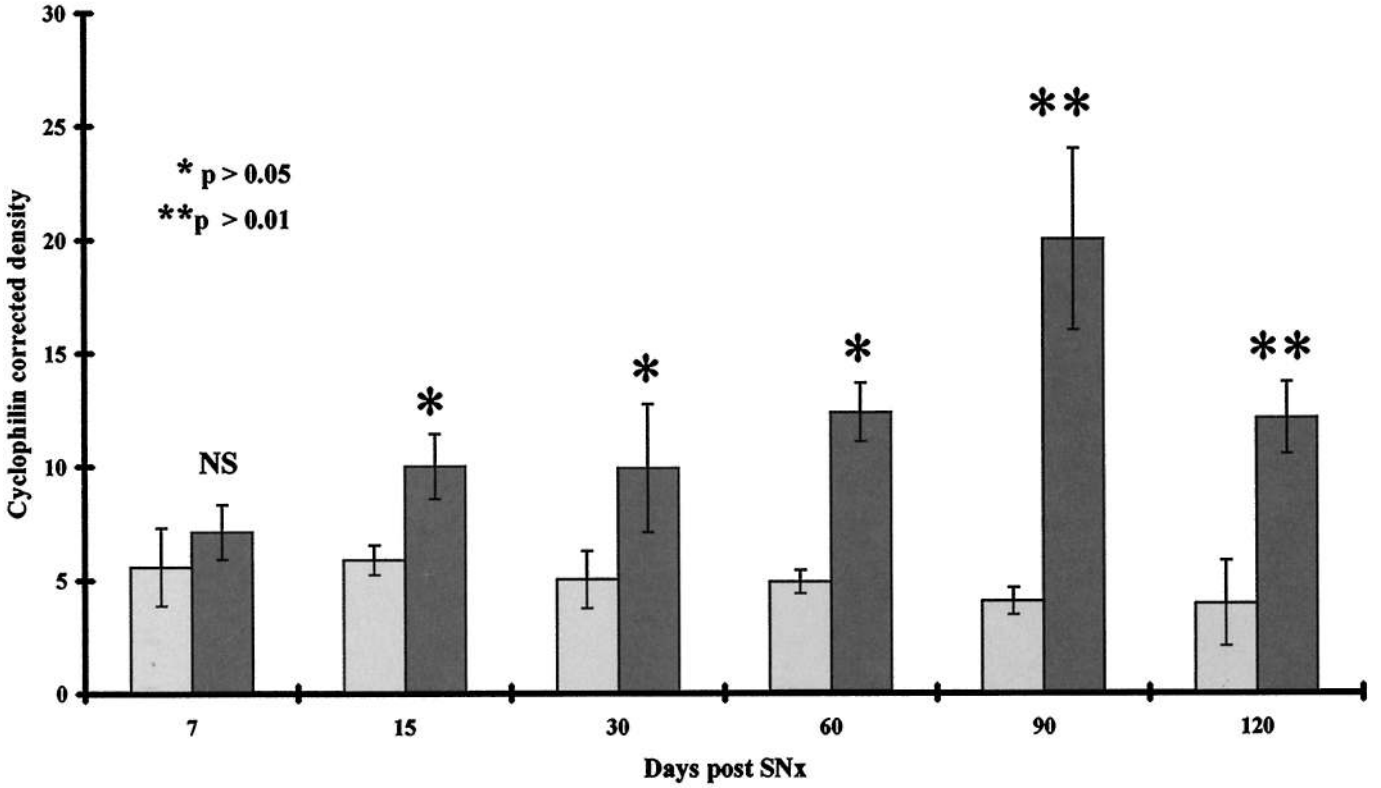

Figure 2. Volume density analysis of the autoradiograph depicted in Figure 1 showing control animals (light bars) and SNx animals (dark bars). Data represent mean density (arbitrary units) ± SEM corrected for loading by a repeat probing with cyclophilin. $n \geq 5$.

Statistical Analyses

Data analyses were performed using one-way ANOVA and *t* test. $P < 0.05$ was taken as significant in both tests. All tests were performed on Microsoft Excel 97.

Results

General Observations

SNx rats demonstrated a steady increase in proteinuria and serum creatinine with time (Table 1), indicating progressive renal insufficiency as documented previously (11) in our earlier studies using this model. All rats survived the SNx and the experimental time course. The level of kidney fibrosis rose steadily throughout the experimental time course showing severe scarring by day 90 post-SNx (Table 1). Mean tubular and glomerular scarring indices were comparable at each time point ($r = 0.95$, $P < 0.001$). Both proteinuria and serum creatinine showed a strong correlation with overall renal scarring ($r = 0.99$, $P < 0.0001$, and $r = 0.82$, $P < 0.01$, respectively). Creatinine clearance in SNx animals became progressively lower than control animals with the development of renal scarring.

tTg mRNA Levels

The autoradiograph in Figure 1 clearly shows that tTg mRNA levels in SNx remnant kidneys are increased compared to controls as early as day 7 post-SNx. These remain elevated throughout the experimental period. Densitometric analysis of the autoradiograph corrected for loading using the housekeeping gene cyclophilin (Figure 2) shows a nonsignificant 27% increase in tTg mRNA at day 7 in the SNx rat. The increase in the SNx animal reaches significance by day 15 post-SNx (+70%, $P < 0.05$) and steadily rises (day 30: +97%, $P < 0.05$; day 60: +151%, $P < 0.05$), reaching a peak at 90 d post-SNx with a 351% increase over controls ($P < 0.01$). Levels remain elevated at 120 d post-SNx. Control animals show a small but nonsignificant decrease in tTg mRNA over the 120-d experimental period.

tTg mRNA Location

In situ hybridization using an antisense construct to tTg showed no detectable binding to either glomeruli (Figure 3D) or tubules in both the cortical (Figure 3A) and medullary

Figure 3. In situ hybridization for tTg. Representative photomicrographs from normal and scarred kidneys (day 90 post-SNx) subjected to *in situ* hybridization studies using sense and antisense digoxigenin-labeled RNA probes specific for tTg. Panel P (scarred kidney) is probed with a sense construct, with all remaining panels probed with an antisense construct. Panels A, D, F, and I are from control kidneys, and all other panels are from scarred kidneys. Panels F through J are from the medulla, and the other panels are from the cortex.

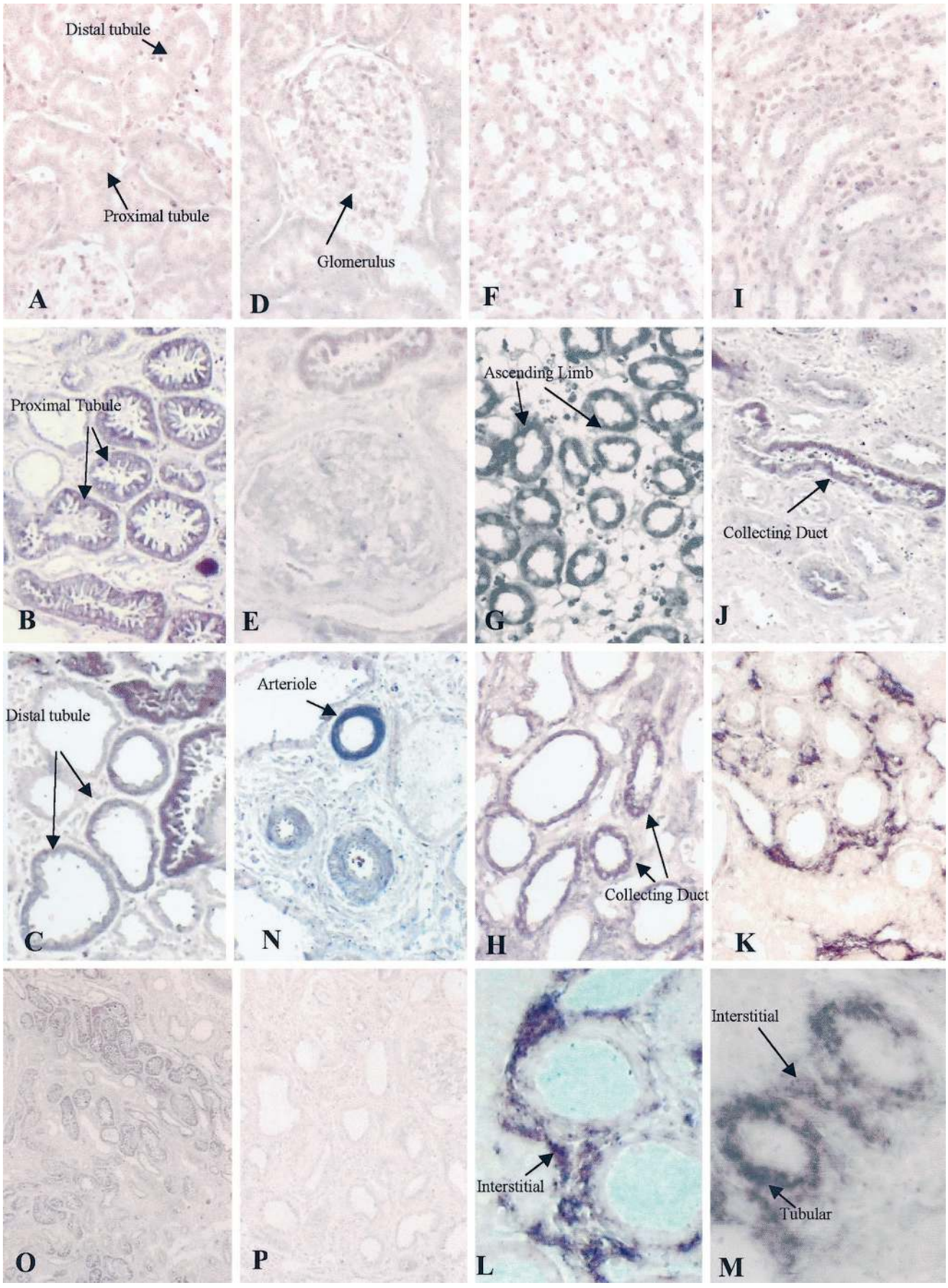
Distal tubule
Proximal tubule
A
Glomerulus
D
F
I
Proximal Tubule
B
E
Ascending Limb
G
Collecting Duct
J
Distal tubule
C
Arteriole
N
Collecting Duct
H
K
O
P
Interstitial
L
Interstitial
Tubular
M

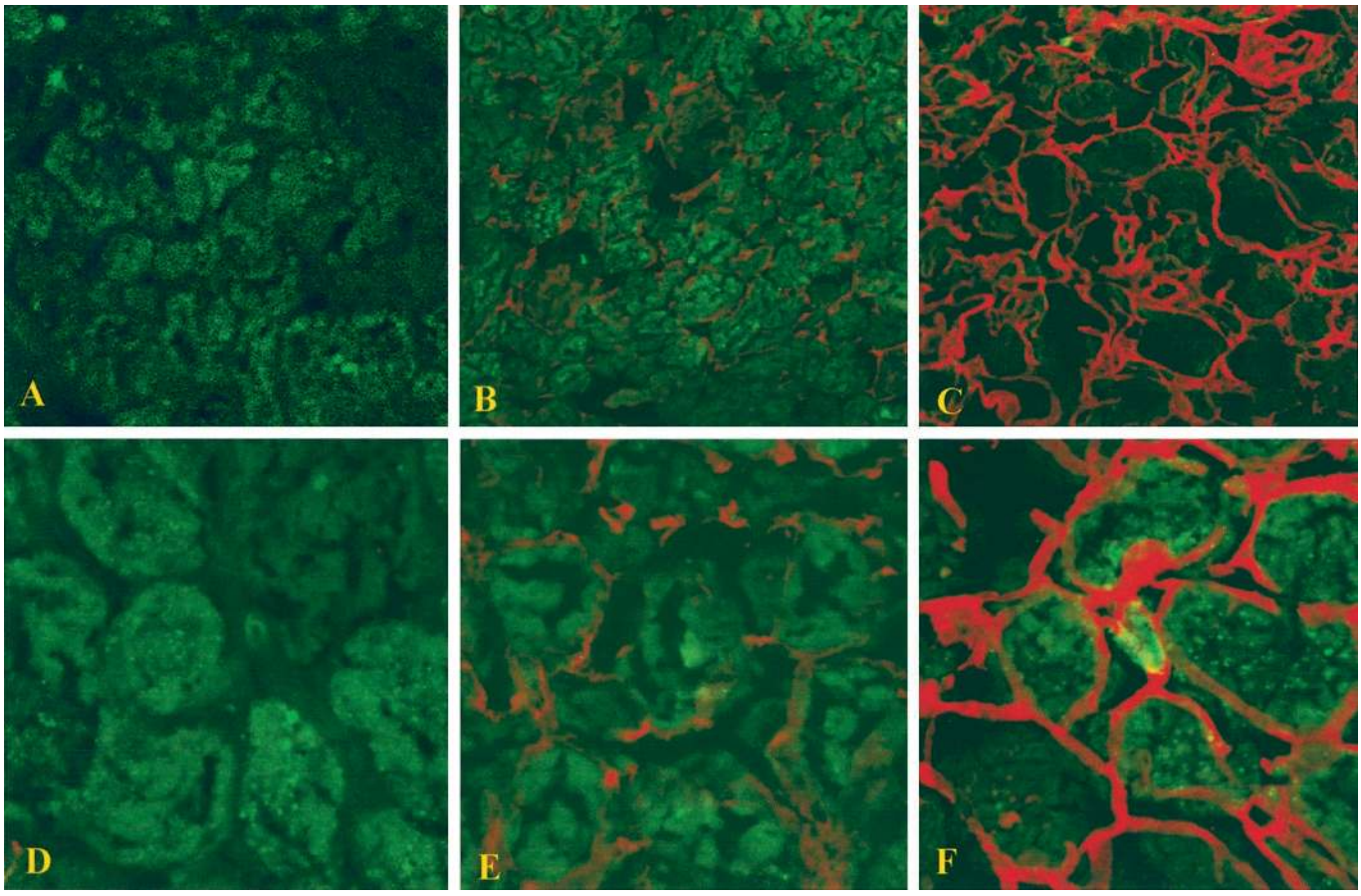

Figure 4. Immunohistochemistry for tTg. Representative photomicrographs from normal (Panels B and E) and scarred kidneys at day 90 post-SNx (Panels C and F) stained for tTg and revealed using a cy5 fluorochrome emission at 665 nm (red) measured by confocal microscopy. Panels A and D represent scarred kidneys probed with nonimmune serum. Panels A through C are shown at low magnification (×160), whereas Panels D through F are viewed at high power (×400).

(Figure 3, F and I) compartments within the development period used. In scarred kidneys (day 90 or later post-SNx), extensive staining was detected in the majority of proximal tubular cells (Figure 3B) and to a lesser extent in distal tubules (Figure 3C), the relative levels of which can be seen at lower magnification (Figure 3O). No increase in the glomerular expression of tTg was detectable in glomeruli in SNx kidneys (Figure 3E). Although staining was predominantly observed in the cortex, there was also some increase in tTg mRNA detected in the medulla, where pockets of what appear to be the ascending limb of the loop of Henle and the occasional collecting duct displayed strong staining (Figure 3, G, H, and J). In some sections of scarred SNx kidneys, the identification of tubular segments was made difficult by the degree of tubular atrophy and tubular dilation, a problem compounded by the nature of this technique.

tTg mRNA could also be found raised in some of the cells constituting the expanding tubular interstitium in terms of both stain frequency and density, although this is best described as sporadic rather than a uniform expression throughout the interstitium. Although this staining typically was seen in areas where elevated tubular expression was seen (Figure 3M), it also occurred independently of tubular expression (Figure 3, K and L). We believe that these cells are fibroblasts, because a similar staining pattern is obtained with α-smooth muscle staining as reported previously by us in this model (37). We also detected tTg mRNA in blood vessels (Figure 3N), but this did not appear to change from that detected in the controls. Probings performed at the same time on consecutive sections using a sense probe to tTg failed to show any binding at all to SNx tissue.

tTg Protein Location

Immunohistochemical analysis of tTg on blocked, unfixed cryostat sections revealed areas of tissue where tTg is strongly bound to the renal architecture. Staining with a nonimmune mouse serum on SNx tissue demonstrates no significant staining (Figure 4, A and D). When this was repeated on normal kidney tissue with a specific anti-tTg monoclonal antibody (CUB7402), there was widespread low-level staining (Figure 4B), which when viewed at higher magnification (×400) is clearly in the extracellular environment (Figure 4E). An increase in the serum content of the blocking buffer to 10% from 5% or the addition of fibronectin at 20 μg/ml did not alter this staining, indicating that the interstitial staining is unlikely to be from nonspecific binding of enzyme released during incubation

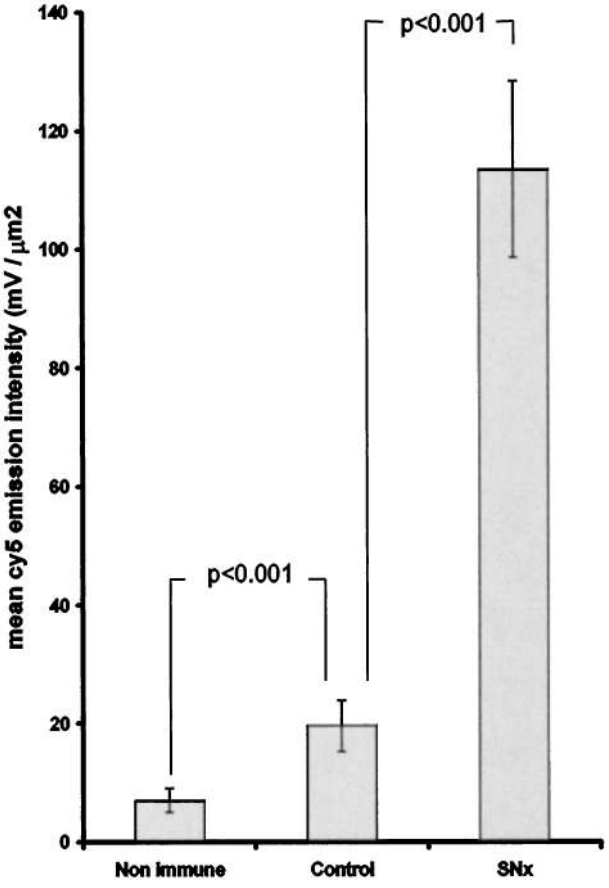

Figure 5. Quantification of the cy5 emission intensity at 665 nm (*i.e.*, tTg antigen) from the confocal microscopy pictures in Figure 4. Data represent mean intensity ± SEM. Analysis is from a minimum of 10 fields (×160 magnification) from at least three individual kidneys per group.

of sections since this would have been absorbed to the fibronectin in the serum. In scarred, 90-d post-SNx remnant kidneys, there is a large increase in the level of tTg antigen found (Figure 4C) that is obviously in the expanding ECM (Figure 4F) when viewed at high magnification (×400). Semiquantification of this increase in tTg antigen staining by measuring the emission intensity of the Cy5 label at 665 nm showed a significant increase in the SNx compared with controls, rising from 19 ± 6 to 116 ± 19 mV/μm^2 ($P < 0.001$) (Figure 5).

Measurement of tTg in Situ Activity

In situ tTg activity assays revealed low incorporation of fluorescein cadaverine (tTg substrate) in normal kidneys (Figure 6D) that could not be localized to any specific renal structure and was not visible when combined with autofluorescence emissions at 530 nm to enable renal morphology to be viewed (Figure 6A). However, in scarred remnant kidneys 90-d post-SNx, incorporation of fluorescein cadaverine was markedly increased (Figure 6, B and E). At 665 nm emission (fluorescein cadaverine [Cy5 label] location only), an image characteristic of ECM staining is generated (Figure 6E), although it is also possible to see lower levels of intracellular tTg activity. With emission monitoring at both 665 and 530 nm, autofluorescence reveals renal morphology, but hides lower levels of tTg activity (Figure 6B). This image suggests that the greatest incorporation of fluorescein cadaverine is peritubular; however, the resolution obtained using this methodology does not allow specific localization to the tubular basement membrane. Interestingly, tTg activity in the expanding ECM (top half of the panel) seems to be concentrated at the periphery of the ECM giving a characteristic "tram line" appearance. There appears to be less tTg activity in the middle of the expanding ECM. Addition of exogenous guinea pig liver tTg to the cryostat incubation medium (100 μg in 50 μl reaction buffer) leads to an increase in the amount of incorporation of fluorescein cadaverine in this area, suggesting that enzyme activity rather than available protein γ-glutamyl groups was the limiting factor (data not shown). Pretreatment of the SNx sections with the tTg inhibitor cystamine (34) removes all fluorescein cadaverine incorporation. Incorporation of fluorescein cadaverine was also reduced if the inactivating tTgase antibody CUB7402 was preincubated with the sections rather than cystamine (data not shown). Semiquantification of Tg activity by measurement of Cy5 emission intensity at 665 nm revealed a sevenfold increase in Tg activity rising from 12.3 ± 1.4 mV/μm^2 in normal animals to 90.4 ± 7.8 mV/μm^2 in 90-d SNx kidneys ($P < 0.0001$) (Figure 7).

Effect of Tg Cross-linking on MMP Degradation of Collagen

Fibril formation was able to incorporate 80.4 ± 1.1% of radiolabeled collagen into the insoluble clot. There was no significant change in the incorporation of radiolabeled collagen if Tg or fibronectin was added to the collagen mixture.

When 10 μg/ml activated purified MMP-1 was added to the insoluble collagen clot and incubated for 16 h at 37°C, it was able to solubilize 84 ± 2.0% of incorporated radiolabeled collagen, compared with 7.4 ± 0.7% purely by incubation alone (Figure 8). When analyzed by polyacrylamide gel electrophoresis, the characteristic band shift obtained after collagenase treatment reported previously by Cawston and Barrett (38) was noted (data not shown). However, when MMP-1 was added to the insoluble clot that was preincubated with tTg for 3 h, the amount of solubilized collagen dropped significantly to 36.6 ± 0.8% of incorporated labeled collagen ($P < 0.0001$) (Figure 8). The addition of 5 mM cystamine (tTg inhibitor) before MMP-1 addition had no significant effect on the amount of collagen solublized from the insoluble clot (40.9 ± 4.2%), indicating that any reductions in solubilized collagen are not due to cross-linking of the MMP-1 by the tTg. Furthermore, if the insoluble clot was allowed to form in the presence of tTg plus fibronectin, then the ability of MMP-1 to degrade collagen was reduced further, since it was only able to solubilize 19.7 ± 1.8% of incorporated labeled collagen.

Measurement of the MMP activity at the end of the experiment using both semiquantitative gelatinase zymography (data not shown) and a fluorogenic substrate for MMP-1 (data not shown) showed no statistical difference between MMP activity

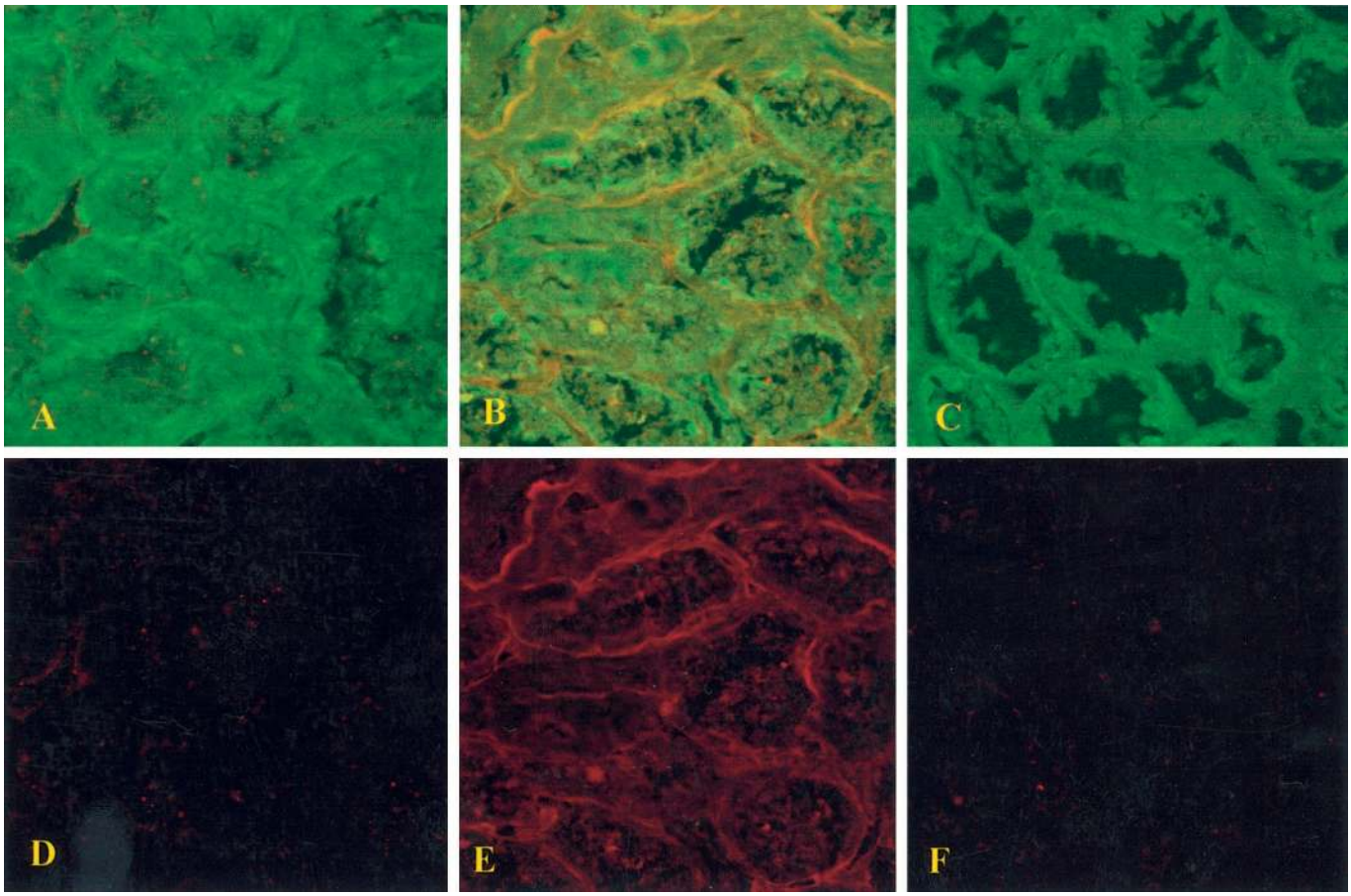

Figure 6. In situ activity for tTg. Representative photomicrographs from normal (Panels A and D) and scarred kidneys at day 90 post-SNx (Panels B, C, E, and F) subjected to *in situ* activity assays for Tg by the incorporation of fluorescein cadaverine and revealed using a cy5 fluorochrome emission at 665 nm (red) measured by confocal microscopy as described in Materials and Methods. Panels C and F represent scarred kidneys pretreated with the Tg antagonist cystamine. Panels A through C represent emissions at both 665 nm (cy5) and 530 nm (tissue autofluorescence), whereas Panels D through F are viewed with emissions at 665 nm (cy5) only.

in any of the groups, further confirming that MMP-1 was not being cross-linked by tTg.

Discussion

In this study, we demonstrate that the previously described alterations in tTg protein expression in the SNx model of renal scarring (11) are a consequence of *de novo* synthesis that commences immediately after SNx and increases steadily as the disease progresses. Moreover, we have shown that renal tubular cells, known to accumulate tTg (11), are also the major site of its synthesis. We have also noted that some of the interstitial cells (which we believe to be fibroblasts) infiltrating the scarred renal interstitium are able to upregulate tTg mRNA production. Importantly, we have been able to detect increasing levels of tTg in the extracellular space, where it is then able to act on the ECM. Furthermore, we have demonstrated that although this enzyme is present throughout the expanding ECM, it appears that the majority of the active form when measured by incorporation of fluorescein cadaverine into cryostat sections is in the ECM with the greatest activity around the basolateral aspect of renal tubules.

Although we have demonstrated intracellular accumulation of tTg in epithelial cells (11), the extracellular localization of this enzyme and its role are yet to be fully clarified. Our findings here confirm its extracellular location in mature rat tissues (39). The previous failure to detect extracellular tTg seems to be one of fixation and/or antibody accessibility. We have been unable to visualize extracellular tTg antigen in paraffin-embedded sections or fixed cryostat sections; however, as demonstrated on unfixed sections, detection is possible. This result is analogous to our previous findings using tTg-transfected Swiss 3T3 fibroblasts whereby extracellular tTg was only detectable when the antibody was added directly to live cells in culture before fixation (13). The extracellular localization of tTg may be the result of a number of mechanisms, the first of which involves leakage of the enzyme from damaged and/or stressed tubular epithelial cells. It is possible that changes to the cell membrane possibly as a result of some type of cell insult could lead to such an externalization of tTg. However, in previous studies using both a human endothelial cell line and mouse Swiss 3T3 fibroblasts, we have presented evidence for the presence of matrix and cell surface-associated enzyme that is not related to leakage via cell rupture (13,27). Externalization of the enzyme could also be the result of the

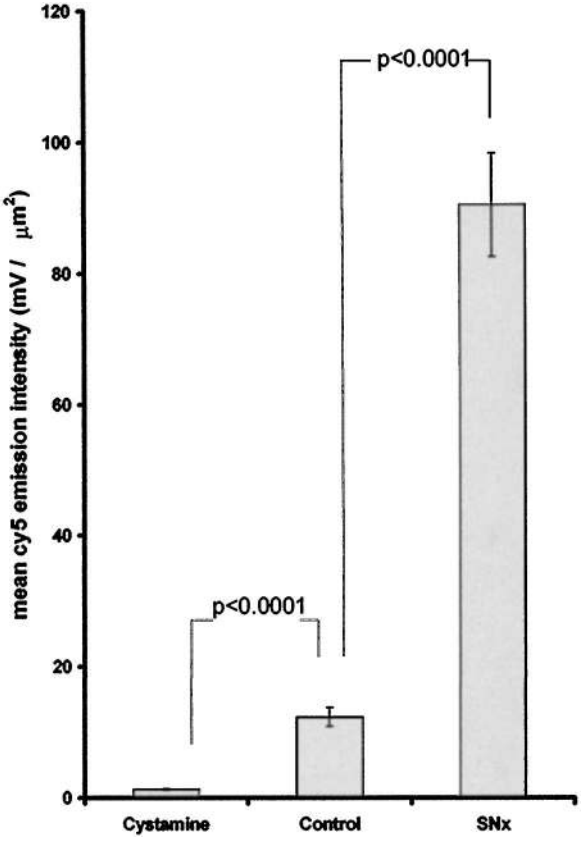

Figure 7. Quantification of the cy5 emission intensity at 665 nm (*i.e.*, tTg activity) from the confocal microscopy pictures in Figure 6. Data represent mean intensity ± SEM. Analysis is from a minimum of 10 fields (×400 magnification) from at least three individual kidneys per group.

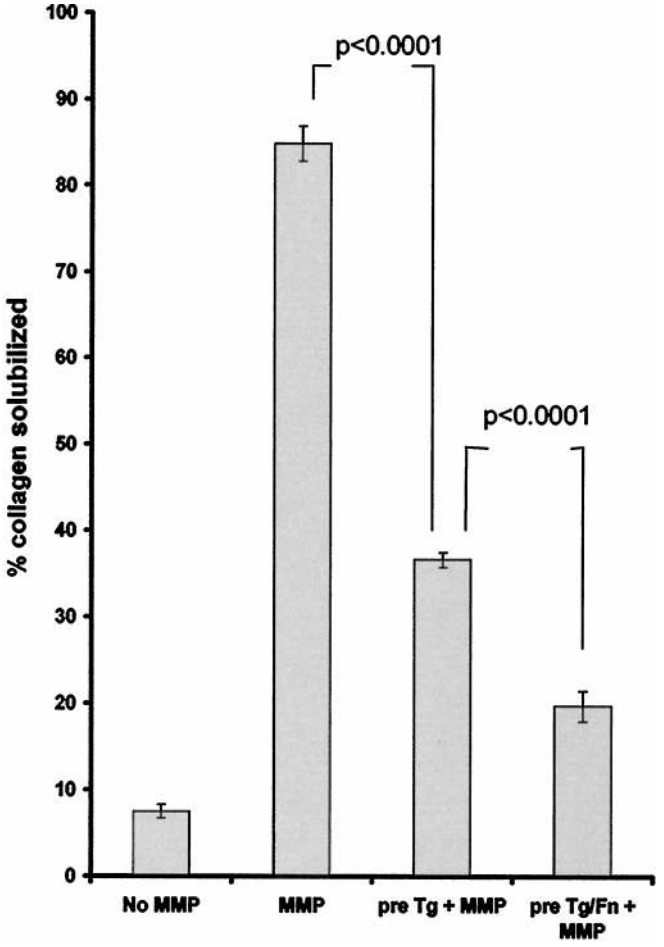

Figure 8. Determination of the ability of matrix metalloproteinase-1 (MMP-1) to digest collagen fibrils by the solubilization of radiolabeled collagen when pretreated with either tTg or tTg and fibronectin. Data represent mean percentage solubilization ± SEM from three experiments.

death of these cells particularly via necrosis, where the cell contents are not maintained as in apoptosis, thus resulting in the spillage of their enzymatic content. This seems unlikely since tTg was detected in the vicinity of apparently healthy tubular cells. Given previous evidence obtained from cells in culture (13,27,40), it seems more likely that the enzyme that has no leader sequence or evidence for its glycosylation (41) is predominantly secreted by a non-Golgi/endoplasmic reticulum route probably via the basal membrane of renal tubular cells. This could explain its concentrated distribution in the vicinity of the peritubular region. However, it cannot be ruled out that the origin of part of the tTg pool is from the interstitial fibroblasts, since some of these cells also show increased expression of the enzyme. The immediate binding to and cross-linking of the proteins in the ECM may also be a mechanism for regulating the enzymes' extracellular activity as judged by the limited amount of incorporated fluorescein cadaverine beyond the peritubular regions.

The upregulation by tubular cells of their synthesis and content of tTg may prove to be a key step in the scarring processes. This enzyme, once elevated and intracellularly activated, can lead to a beneficial stabilizing influence or a detrimental death signal. On one hand, tTg may be involved in wound repair by stabilizing the underlying ECM to compensate for both loss of renal cells and architecture (11), thus maintaining tissue integrity. The detected activity of tTg, which is confined to the tubular basement membrane area, suggests a preferential site of activity consistent with a stabilizing role on peritubular ECM. Such localization of the active enzyme peripheral to the tubular cells is consistent with a role in the deposition of new ECM rather than cross-linking of existing ECM. This is consistent with increasing evidence to indicate the importance of tTg in basement membrane stabilization of both endothelial cells (26) and in epithelial cells such as those found in the embryonic lung, where it has been suggested that tTg may be used to prevent or delay further remodeling by cross-linking the alveolar basement membrane and stabilizing the ECM (39). On the other hand, it has been shown that the excessive accumulation of tTg within renal epithelial cells can lead to their death through extensive intracellular cross-linking of proteins in the absence of apoptosis (11,12). This tTg-mediated death process is dependent on Ca^{2+} influx into the cell as a result of damage, perhaps via ischemic injury as the tubular interstitial fibrosis progresses. However, activation of

tTg is also thought to be a key step in the final events of the apoptotic process, whereby increases in intracellular Ca^{2+} lead to formation of the apoptotic envelope (16,17,22). Conceivably, the level of tTg expression and its subsequent activation may determine its beneficial healing properties or its detrimental death signals.

A role for tTg in the pathogenesis of renal fibrosis has previously been put forward by our initial observations. tTg may influence the renal fibrotic process through various pathways. It may, as we postulated previously, stabilize the ECM through the incorporation of $\epsilon(\gamma$-glutamyl) lysine cross-links (28). Such a bond appears to be resistant to any mammalian enzyme, making it irreversible and resistant to the action of collagenases (15–17). An indication of this was demonstrated in our *in vitro* assay, which clearly indicated that collagen or collagen mixtures including fibronectin become more resistant to MMP breakdown when previously exposed to tTg. The collagen I used in this assay, which is one of the predominant collagens found in the scarring process (42), has previously been shown to have limited lysine amine acceptor sites for tTg cross-linking (43). However, our data clearly show that incubation of the enzyme with this collagen leads to increased resistance to MMP breakdown, indicating that intermolecular cross-links are occurring either between collagen fibrils or between collagen and tTg itself since the enzyme has previously been shown to incorporate itself into the ECM (44). The inclusion of fibronectin into this mixture, which can act as both a lysine acceptor and glutamine donor in tTg cross-linking (27,45), further increased the resistance to MMP breakdown. This ability of tTg cross-linking to increase the resistance of proteins to protease breakdown, which in the damaged kidney is likely to include a greater array of ECM substrates than those tested in an *in vitro* assay, is in keeping with the action of the plasma Tg (factor XIIIa), which cross-links fibrin making it more resistant to the action of proteinases such as plasmin (18). The widely described phenotype of fibrosis of elevated ECM production and decreased ECM degradation due to the reduction of MMP activity can now surely be expanded to include reduced breakdown due to qualitative changes to the ECM as demonstrated in this study. Qualitative changes may in fact prove to be the major reason for reduced degradation of the ECM as suggested by recent studies on atherosclerosis (9), liver fibrosis (10), and kidney fibrosis (11).

The importance of tTg in the stabilization and deposition of the ECM may also be linked directly or indirectly to its role in the incorporation and storage of the transforming growth factor-β1 (TGF-β1)-binding protein LTBP-1. The cross-linking of LTBP-1 to the matrix via tTg has been reported as a necessary step in both the storage and activation of matrix-bound TGF-β1 (46). In our previous studies using the rat SNx model, we have shown an increase in TGF-β1 staining in the interstitium of diseased kidney from day 15 onward (47) in a similar distribution to that observed with tTg. Hence, the amount of matrix-bound TGF-β1, which is dependent on extracellular tTg, could be crucial in determining the extent of progression of the wound-healing/fibrotic response given the reputation of TGF-β1 as one of the most fibrogenic renal growth factors (48).

In conclusion, this study has demonstrated for the first time that the induction of renal fibrosis leads to large changes in the synthesis, activity, and location of tTg. The consequences of these changes both intracellular in renal tubular cell death and extracellular where the enzyme is likely to play important roles both in matrix deposition/stabilization and in the storage and activation of TGF-β1 are likely to have a profound effect on the progression of renal fibrosis. tTg may therefore be a potential novel target in a therapeutic approach aimed at controlling renal scarring and renal failure.

References

1. Floege J, Johnson RJ, Gordon K, Yoshimura A, Campbell C, Iruela-Arispe L, Alpers CE, Couser WG: Altered glomerular extracellular matrix synthesis in experimental membranous nephropathy. *Kidney Int* 42: 573–585, 1992
2. Peten EP, Stricker LJ, Carome MA, Elliott SJ, Yang CW, Striker GE: The contribution of increased collagen synthesis to human glomerulosclerosis: A quantitative analysis of α(2) IV collagen mRNA expression by competitive polymerase chain reaction. *J Exp Med* 176: 1571–1576, 1992
3. Jones CL, Buch S, Post M, McCulloch L, Liu E, Eddy AA: Renal extracellular matrix accumulation in acute purine aminonucleoside nephrosis in rats. *Am J Pathol* 135: 719–733, 1991
4. Eddy AA, Giachelli CM: Renal expression of genes that promote interstitial inflammation and fibrosis in rats with protein overload proteinuria. *Kidney Int* 47: 1546–1557, 1995
5. Matrisian LN: Metalloproteinases and their inhibitor in matrix remodelling. *Trends Genet* 6: 121–125, 1990
6. Griffin M, Smith LL, Wynne J: Changes in transglutaminase activity in an experimental model of pulmonary fibrosis induced by paraquat. *Br J Exp Pathol* 60: 653–661, 1979
7. Bowness JM, Tarr AH, Wiebe RI: Transglutaminase-catalysed cross-linking: A potential mechanism for the interaction of fibrinogen, low density lipoprotein and arterial type III procollagen. *Thromb Res* 54: 357–367, 1989
8. Bowness JM, Tarr AH: Lipoprotein binding of crosslinked type III collagen aminopropeptide and fractions of its antigen in blood. *Biochem Biophys Res Commun* 170: 519–524, 1990
9. Bowness JM, Venditti M, Tarr AH, Taylor JR: Increase in epsilon (gamma-glutamyl) lysine crosslinks in atherosclerotic aortas. *Atherosclerosis* 111: 247–253, 1994
10. Mirza A, Liu SH, Frizell E, Zhu J, Maddukuri S, Martinez J, Davies P, Schwarting R, Norton P, Zern MA: A role for tissue transglutaminase in hepatic injury and fibrogenesis, and its regulation by NF$\kappa\beta$. *Am J Physiol* 272: G281–G288, 1997
11. Johnson TS, Griffin M, Thomas GL, Skill JN, Cox A, Nicholas B, Birckbichler PJ, Muchaneta-Kubara C, El-Nahas AM: The role of transglutaminase in the rat subtotal nephrectomy model of renal fibrosis. *J Clin Invest* 99: 2950–2960, 1997
12. Johnson TS, Scholfield CI, Parry J, Griffin M: Induction of tissue transglutaminase by dexamethasone: Its correlation to receptor number and transglutaminase mediated cell death in a series of malignant hamster fibrosarcomas. *Biochem J* 331: 105–112, 1998
13. Verderio E, Nicholas B, Gross S, Griffin M: Regulated expression of tissue transglutaminase in Swiss 3T3 fibroblasts: Effects on the processing of fibronectin, cell attachment, and cell death. *Exp Cell Res* 239: 119–138, 1998

14. Folk JE, Finlayson JE: The $\epsilon(\gamma$-glutamyl) lysine crosslink and the catalytic role of transglutaminase. *Adv Protein Chem* 31: 1–133, 1977
15. Folk JE: Transglutaminases. *Ann Rev Biochem:* 49: 517–531, 1980
16. Fesus L, Thomazy V, Autuori F, Ceru MP, Tarcsa E, Piacentini M: Apoptotic hepatocytes become insoluble in detergents and chaotropic agents as a result of transglutaminase action. *FEBS Lett* 245: 150–154, 1989
17. Fesus L, Davies PJA, Piacentini M: Apoptosis: Molecular mechanisms in programmed cellular death. *Eur J Cell Biol* 56: 170–177, 1991
18. Lorand L, Conrad SM: Transglutaminases. *Mol Cell Biochem:* 58: 9–35, 1984
19. Rice RH, Green H: The cornified envelope of terminally differentiated human epidermal keratinocytes consists of cross linked protein. *Cell* 11: 417–422, 1977
20. Greenberg CS, Birckbichler PJ, Rice RH: Transglutaminases: Multifunctional enzymes that stabilise tissues. *FASEB J* 5: 3071–3077, 1991
21. Fesus L, Thomazy V, Falus A: Induction and activation of tissue transglutaminase during programmed cell death. *FEBS Lett* 224: 104–108, 1987
22. Knight CRL, Rees RC, Griffin M: Apoptosis: A potential role for cytosolic transglutaminase and its importance in tumour progression. *Biochim Biophys Acta* 1096: 312–318, 1991
23. Knight CRL, Hand D, Piacentini M, Griffin M: Characterisation of the transglutaminase-mediated large molecular weight polymer from rat liver: Its relationship to apoptosis. *Eur J Cell Biol* 60: 210–216, 1993
24. Cai D, Ben T, De Luca LM: Retinoids induce tissue transglutaminase in NIH-3T3 cells. *Biochem Biophys Res Commun* 175: 1119–1124, 1991
25. Bowness JM, Folk JE, Timpl R: Identification of a substrate for liver transglutaminase on the aminopropeptide of type III collagen. *J Biol Chem* 262: 1022–1024, 1987
26. Aeschlimann D, Paulsson M: Crosslinking of laminin. Nidogen complexes by tissue transglutaminase: A novel mechanism for basement membrane stabilisation. *J Biol Chem* 266: 15308–15817, 1991
27. Jones RA, Nicholas B, Mian S, Davies PJA, Griffin M: Reduced expression of tissue transglutaminase in a human endothelial cell line leads to changes in cell spreading, cell adhesion and reduced polymerisation of fibronectin. *J Cell Sci* 110: 2461–2472, 1997
28. Kleman JP, Aeschlimann D, Paulsson M, van der Rest M: Transglutaminase: Catalysed cross linking of fibrils of collagen V/XI in A204 rhabdomyosarcoma cells. *Biochemistry* 34: 13768–13775, 1995
29. Knight CRL, Rees RC, Elliott BM, Griffin M: The existence of an inactive form of transglutaminase within metastasizing tumours. *Biochim Biophys Acta* 1053: 13–20, 1990
30. Chung SI, Chang SK, Cocuzzi ET, Folk JE, Kim HC, Lee SY, Maartine TN, Nigra T, Sun HS: *Advances in Post Translational Modification of Proteins and Aging*, edited by Zappia V, Galletti P, Porta R, Wold F, New York and London, Plenum, 1988
31. Bowness JM, Tarr AH, Wong T: Increased transglutaminase activity during skin wound healing in rats. *Biochim Biophys Acta* 967: 234–240, 1988
32. Lorand L, Parameswaran KN, Velasco PT, Hsu LK, Seifring GE Jr: New colored and fluorescent amine substrates for activated fibrin stabilizing factor (Factor XIIIa) and for transglutaminase. *Anal Biochem* 131: 419–425, 1983
33. Werb Z, Burleigh MC: Collagen fibril assay. *Biochem J* 137: 373–385, 1974
34. Smethurst PA, Griffin M: Measurement of tissue transglutaminase activity in a permeabilized cell system: Its regulation by Ca^{2+} and nucleotides. *Biochem J* 313: 803–808, 1996
35. Herron GS, Banda MJ, Clark EJ, Gavrilovic J, Werb Z: Secretion of metalloproteinases by stimulated capillary endothelial-cells: Expression of collagenase and stromelysin activities is regulated by endogenous inhibitors. *J Biol Chem* 261: 2814–2818, 1986
36. Berman J, Green M, Sugg E, Anderegg R, Millington DS, Norwood DL, Mcgeehan J, Wiseman J: Rapid optimisation of enzyme substrates using defined substrate mixtures. *J Biol Chem* 267: 1434–1437, 1992
37. Muchaneta-Kubara EC, El Nahas AM: Myofibroblast phenotypes expression in experimental renal scarring. *Nephrol Dial Transplant* 12: 904–915, 1997
38. Cawston TE, Barrett AJ: A Rapid and reproducible assay for collagenase using [1-^{14}C]-acetylated collagen. *Anal Biochem* 99: 340–345, 1979
39. Schittny JC, Paulsson M, Vallan C, Burri PH, Kedei N, Aeschlimann D: Protein cross-linking mediated by tissue transglutaminase correlates with the maturation of extracellular matrices during lung development. *Am J Respir Cell Mol Biol* 17: 334–343, 1997
40. Lajemi M, Demignot S, Adolphe M: Detection and characterisation, using fluorescein cadaverine, of amine acceptor protein substrates accessible to active transglutaminase expressed by rabbit articular chondrocytes. *Histochem J* 30: 499–508, 1998
41. Gentile V, Saydak M, Chiocca EA, Akande O, Birckbichler PJ, Lee KN, Stein JP, Davies PJA: Isolation and characterisation of cDNA clones to mouse macrophage and human endothelial-cell tissue transglutaminases. *J Biol Chem* 266: 478–483, 1991
42. Hewitson TD, Darby IA, Bisucci T, Jones CL, Becker GJ: Evolution of tubulointerstitial fibrosis in experimental renal infection and scarring. *J Am Soc Nephrol* 9: 632–642, 1998
43. Bowness JM, Folk JE, Timpl R: Identification of a substrate site for liver transglutaminase on the aminopropeptide of type III collagen. *J Biol Chem* 262: 1022–1024, 1987
44. Barsigian C, Stern AM, Martinez J: Tissue (type II) transglutaminase covalently incorporates itself, fibrinogen, or fibronectin into high molecular weight complexes on the extracellular surface of isolated hepatocytes. *J Biol Chem* 266: 22501–22509, 1991
45. Martinez J, Chalupowicz DG, Roush RK, Sheth A, Barsigian C: Transglutaminase-mediated processing of fibronectin by endothelial-cell monolayers. *Biochemistry* 33: 2538–2545, 1994
46. Kojima S, Nara K, Rifkin D: Requirement for transglutaminase in the activation of latent transforming growth factor β in bovine endothelial cells. *J Cell Biol* 121: 439–448, 1993
47. Muchaneta-Kubara EC, Sayed-Ahmed N, El Nahas AM: Subtotal nephrectomy: A mosaic of growth factors. *Nephrol Dial Transplant* 10: 320–327, 1995
48. Border WA, Noble NA: TGF-β1 in kidney fibrosis: A target for gene therapy. *Kidney Int* 51: 1388–1396, 1997